Influence of coating material on laser damage threshold of TiO_2 films

Jianke Yao (姚建可), Zhengxiu Fan (范正修), Hongbo He (贺洪波), and Jianda Shao (邵建达)

R&D Center for Optical Thin Film Coatings, Shanghai Institute of Optics and Fine Mechanics, Chinese Academy of Sciences, Shanghai 201800

Received March 21, 2007

The optical property, structure, surface properties (roughness and defect density) and laser-induced damage threshold (LIDT) of TiO_2 films deposited by electronic beam (EB) evaporation of TiO_2 (rutile), TiO_2 (anatase) and $TiO_2 + Ta_2O_5$ composite materials are comparatively studied. All films show the polycrystalline anatase TiO_2 structure. The loose sintering state and phase transformation during evaporating TiO_2 anatase slice lead to the high surface defect density, roughness and extinction coefficient, and low LIDT of films. The $TiO_2 + Ta_2O_5$ composite films have the lowest extinction coefficient and the highest LIDT among all samples investigated. Guidance of selecting materials for high LIDT laser mirrors is given.

OCIS codes: 310.3840, 140.3330.

In high-power laser applications, one of the factors preventing its development is the low laser-induced damage threshold (LIDT) of dielectric coatings[1]. The performance (high reflectance/transmittance and LIDT) of device is strongly influenced by the evaporation material[2]. TiO_2 is a hard, durable, and laser-damage-resistant material with high refractive index and is widely used to produce multilayer coatings in the visible spectral region[3]. The surface defects are the damage initiation of laser coatings[4] and scatter center in TiO_2 films[5]. The defects concentration is also determined by the evaporation materials[6]. TiO_2 occurs naturally as the minerals rutile and anatase forms, which are often used to obtain nonabsorbing TiO_2 films[7]. The optical and surface characteristics of films can also be improved by using TiO_2+Ta_2O_5 composite coating materials[8]. The main aim of this paper is to comparatively study the optical property, structure, surface properties (roughness and defect density), and LIDT of films deposited by above three coating materials.

In our experiment, all films are deposited by the electronic beam (EB) evaporation. High-quality BK7 substrates are cleaned ultrasonically in an alcohol solution before deposition. The coating materials with their sintering state before deposition and sample number are shown in Table 1. The process parameters of all deposited films are as follows. The physical thickness of single layer films is about 550 nm. The substrate temperature is kept at 350 °C during deposition. The base pressure is 2×10^{-3} Pa before deposition and the oxygen partial pressure is 3×10^{-2} Pa during deposition. The deposition rate is 1.33 nm/s. The samples are annealed at 400°C in air for 24 h after deposition.

Table 1. Samples in Our Experiment

Sample No.	Coating Material	Sintering State	Annealing Temperature (°C)
1	TiO_2 (Rutile)	Black Dense Granule	As-Deposited
2			400
3	TiO_2 (Anatase)	White Loose Slice	As-Deposited
4			400
5	$TiO_2 + Ta_2O_5$ (Weight 7:3)	Black Dense Granule	As-Deposited
6			400

The transmittance spectra of films are measured with a Lambda 900 spectrometer. Refractive index n and extinction coefficient k of films are determined from the transmittance spectrum with the envelope method[9]. The crystal structure of films is investigated by a RGAKU/MAX-3C X-ray diffraction (XRD) meter. Data are gathered over angular range from $2\theta = 10° - 90°$. The X-ray source used is Cu $K\alpha$ radiation at the wavelength of 0.15418 nm. Grain size C of anatase TiO_2 in terms of full-width at half-maximum (FWHM) B of crystal plane (101) is calculated using the relation $C = 0.89\lambda/B\cos\theta$[1]. The surface defects are detected by Nomarski microscope. The root-mean-square (RMS) surface roughness is measured by the total integrated scattering method [10]. LIDT is tested using a 1064-nm, 120-ns pulse laser in the 1-on-1 mode with the ISO standard 11254-1[11].

Figure 1 shows the selected transmittance spectra of samples. It is found that the spectrum of $TiO_2 + Ta_2O_5$

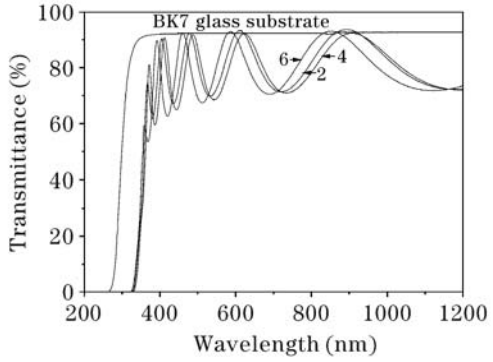

Fig. 1. Selected transmittance spectra of samples.

composite film after annealing shifts to the short wavelength region and has the lowest short-wavelength edge. The spectrum of film using TiO_2 anatase coating material after annealing shifts to right and the transmittance maximum is less than that of the film using TiO_2 rutile coating material after annealing.

Table 2 shows the calculated optical constants of films. The films using TiO_2 rutile coating material have the highest refractive index and intermediate extinction coefficient. The refractive index decreases slightly and extinction coefficient increases dramatically for the films using TiO_2 anatase coating material. The $TiO_2 + Ta_2O_5$ composite film has the lowest refractive index and extinction coefficient. The refractive index increases and extinction coefficient decreases after annealing.

Figure 2 shows the XRD spectra of samples. All films show the polycrystalline anatase TiO_2 structure. We find no Ta_2O_5 crystal diffraction peaks in the $TiO_2 + Ta_2O_5$ composite films. The calculated grain size of anatase TiO_2 is shown in Table 3. The $TiO_2 + Ta_2O_5$ composite films have the minimum grain size. The grain size increases to maximum for films using TiO_2 anatase coating material and annealing.

The measured surface defect density, RMS roughness, and LIDT of films are also shown in Table 3. The films using TiO_2 anatase coating material have the highest surface defect density and roughness and the lowest LIDT. The $TiO_2 + Ta_2O_5$ composite films show reduced surface defect density and roughness and the highest LIDT. The surface defect density, roughness, and LIDT increase after annealing. From Tables 2 and 3, it is found that the films with low grain size have low surface defect density and roughness, and the films with low (high) extinction coefficient and surface defect density have high (low) LIDT.

Table 2. Calculated Optical Constants of Films

Sample	$\lambda = 532$ nm		$\lambda = 800$ nm		$\lambda = 1064$ nm	
No.	n	k ($\times 10^{-4}$)	n	k ($\times 10^{-4}$)	n	k ($\times 10^{-4}$)
1	2.27	5.50	2.17	1.20	2.16	0.60
2	2.27	3.40	2.19	0.01	2.18	0.00
3	2.24	17.20	2.14	9.20	2.12	6.80
4	2.25	7.00	2.16	4.60	2.14	3.70
5	2.21	0.40	2.13	0.01	2.12	0.00
6	2.24	0.20	2.15	0.00	2.13	0.00

Table 3. Calculated Grain Size C of Anatase TiO_2, Measured Surface Defect Density ρ, RMS Roughness σ, and LIDT of Films

Sample No.	1	2	3	4	5	6
C (nm)	33.9	41.4	49.6	50.9	22.5	25.6
ρ (mm^{-2})	25	68	160	250	18	21
σ (nm)	2.70	2.93	3.34	6.93	2.66	2.80
LIDT ($J \cdot cm^{-2}$)	9.0	9.7	7.0	8.0	10.1	11.3

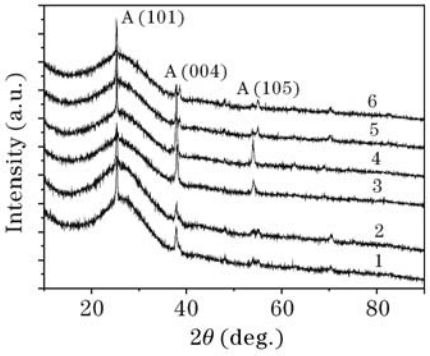

Fig. 2. XRD spectra of samples.

The refractive index is closely related to the electronic polarizability of ions and the local field inside the material. Ta_2O_5 has lower refractive index than TiO_2 due to their position of the metal in the periodic table. Cation replacement of Ti^{4+} by Ta^{5+} in the $TiO_2 + Ta_2O_5$composite films causes the decrease of refractive index.

Extinction coefficient is influenced by absorption and scattering coefficient. The scattering of a rough surface is in general proportional to the square of RMS roughness[12]. In the optical transparency region of a material the short-wavelength edge λ, determined by the electronic transitions across the band gap, is the qualitative indication of the degree of absorption. The band gap of Ta_2O_5 is larger than that of TiO_2, therefore the TiO_2+Ta_2O_5 composite films have lower absorption than those of TiO_2 films. It is reported[12] that the polycrystalline structure has larger scattering than that of amorphous phase. The as-deposited Ta_2O_5 film is always amorphous in structure and has a sluggish and reversible phase transformation near 1360 °C[8]. The anatase phase is a low-temperature polymorph with a loose structure and will transfer to a thermodynamically stabler and denser rutile phase near 1100 °C during evaporation[13]. The phase transition causes particles to be ejected from the source because of stress relief. Moreover the loose anatase slice will contain more gas in the voids of slice during the sintering process. During EB evaporation, the intense heat may cause the entrapped gases to explosively break out of the slice and send particles toward the substrate. Therefore the films using TiO_2 anatase coating material have the highest surface defect density and roughness, which also increase the scattering and extinction coefficient and lower the LIDT of films. The highest LIDT of $TiO_2 + Ta_2O_5$ composite films is caused by their lowest absorption (extinction coefficient) and surface defect density. The crystal growth after annealing increases the surface defect density and roughness. The improved LIDT after annealing is mainly due to the decrease of the absorption (extinction coefficient) during annealing.

In conclusion, the rutile is thermodynamically stable and dense phase to inhibit phase change and material ejection, which lower the defect generation during evaporation. Doping with Ta_2O_5 can decrease the extinction coefficient of films. Surface defects and extinction coefficients are key factors influencing the absorption of films. Generally, the film with low absorption have high LIDT.

This work was supported by the National Natural Science Foundation of China under Grant No. 60608020. J. Yao's e-mail address is yjk@siom.ac.cn.

References

1. J. Yao, J. Shao, H. He, and Z. Fan, Appl. Surf. Sci. **253,** 8911 (2007).
2. K. N. Rao, Opt. Eng. **41,** 2357 (2002).
3. J. Yao, Z. Fan, Y. Jin, Y. Zhao, H. He, and J. Shao, Thin Solid Films (to be published) (2007).
4. J. Yao, H. Li, Z. Fan, Y. Tang, Y. Jin, Y. Zhao, H. He, and J. Shao, Chin. Phys. Lett. **24,** 1964 (2007).
5. N. Albertinetti and H. T. Minden, Appl. Opt. **35,** 5620 (1996).
6. R. Chow, S. Falabella, G. E. Loomis, F. Rainer, C. J. Stolz, and M. R. Kozlowski, Appl. Opt. **32,** 5567 (1993).
7. H. K. Pulker, G. Paesold, and E. Ritter, Appl. Opt. **15,** 2986 (1976).
8. C. C. Lee and C. J. Tang, Appl. Opt. **45,** 9125 (2006).
9. R. Swanepoel, J. Phys. E **16,** 1214 (1983).
10. H. Hou, K. Yi, S. Shang, J. Shao, and Z. Fan, Appl. Opt. **44,** 6163 (2005).
11. ISO 11254-1, *Lasers and laser-related equipment — Determination of laser-induced damage threshold of optical surfaces — Part 1: 1-on-1 test* (2002).
12. W. H. Wang and S. Chao, Opt. Lett. **23,** 1417 (1998).
13. J. Yao, J. Shao, H. He, and Z. Fan, Vacuum **81,** 1023 (2007).